

A fluorescent probe for the imaging of nitroreductase with signal amplification in high-viscosity environments

Yunfan Liu, Jiaying Li, Hongjin Huang and Yang Shu*

Department of Chemistry, College of Sciences, Northeastern University, Box 332,
Shenyang 110819, China

*Corresponding Authors

*E-mail address: shuyang@mail.neu.edu.cn (Shu).

Materials and chemicals

2-methyl benzothiazole, 4-(Dimethylamino)cinnamaldehyde, Quinine sulfate dihydrate, Nicotinamide adenine dinucleotide (NADH) disodium salt, and dicoumarol were acquired from Bide Pharmatech Ltd (Shanghai). Pyridine and the silica gel of 200-400 mesh (the sorbent of column chromatography) were acquired from Sinopharm (Shenyang) Chemical Reagent Co., Ltd. Iodoethane, Glycerol, Dimethyl sulfoxide (DMSO), Rhodamine B, the metal chloride, sodium salt with various anions, and amino acids used in the selectivity evaluation were received from Aladdin (Shanghai) Reagent Co., Ltd. All other inorganic salts were commercially available from Aladdin Reagent Co., Ltd. The solvents used were acquired from Shanghai Titan Scientific Co., Ltd. Lipopolysaccharide (LPS), Nitroreductase (NTR) and other enzymes used in the selectivity evaluation were received from Sigma-Aldrich. Mito-Tracker Green and adenosine triphosphate (ATP) were acquired from Beyotime Biotech. Inc. All the reagents/chemicals and solvents were at least of analytical-reagent or HPLC grade and used without further purification. 3-(4,5-Dimethylthiazol-2-yl) -2,5-diphenyltetrazolium bromide (MTT) assay kits were acquired from KeyGEN Biotech Co., Ltd (Nanjing, China). MGC Anaero Pack™ C-1, C-2, and AnaeroPack™ 2.5L Rectangular Jar were commercially available from Mitsubishi Gas Chemical Company, Inc. SH-SY5Y cell lines were received from Shanghai Zhong Qiao Xin Zhou Biotechnology Co., Ltd. A549 and HeLa cell lines were obtained from the National Collection of Authenticated Cell Cultures (China).

Instrumentation

Deionized water with a resistivity of $18.2 \text{ M}\Omega \cdot \text{cm}^{-1}$ (25°C) was acquired on a Milli-Q water purification system (Millipore) and used throughout the experiments. ^1H NMR (400 MHz) and ^{13}C NMR (151 MHz) spectra were recorded on a Bruker NMR spectrometer (Bruker Biospin, Switzerland). DMSO- d_6 and Methanol- d_4 were used as the solvents, and tetramethylsilane (TMS) as an internal reference standard. An ESI mass spectrometer (PerkinElmer, America) was employed for measuring the mass spectra. UV-vis absorption spectra were recorded on a U-3900 UV-vis spectrophotometer. Fluorescence spectra were measured by an RF-6000 fluorescence spectrophotometer (Shimadzu, Japan). Fluorescence imaging in live cells was conducted with an FV-1200 confocal laser scanning microscope (CLSM) (Olympus, Japan).

Preparation and characterization

ENBT and EBT were prepared according to the synthetic route in Scheme 1.

Synthesis of ENBT. 4-(Dimethylamino)cinnamaldehyde (0.21 g, 1.2 mmol) was dissolved in 15 mL of methanol. Then, an appropriate amount of 2-methyl benzothiazole (0.305 g, 1.0 mmol) was added and the solution was stirred at room temperature for 5 min. Pyridine (0.25 mL) was then added and the resulting solution was heated and stirred at 70°C overnight (~ 12 h). After completion of the reaction,

the reaction mixture was cooled to room temperature and concentrated under vacuum. Ethyl acetate (10 mL) was added to the resulting dark liquid and the product at the bottom of the flask precipitated as a dark-colored solid. After precipitation of the solution for 30 min, the solid obtained was collected by filtration under reduced pressure. The solid was washed 3 times with ethyl acetate (5 mL) and the desired product ENBT (0.33 g, 71%) was collected. ¹H NMR (400 MHz, DMSO-d₆) δ 8.47 (d, J = 8.0 Hz, 1H), 8.34 (d, J = 9.8 Hz, 2H), 8.31 (s, 1H), 8.09 (dd, J = 14.9, 10.0 Hz, 1H), 7.92 (s, 1H), 7.89 (d, J = 9.7 Hz, 2H), 7.85 – 7.74 (m, 2H), 7.71 – 7.52 (m, 2H), 4.85 (q, J = 7.1 Hz, 2H), 1.48 (t, J = 7.1 Hz, 3H). ¹³C NMR (101 MHz, DMSO-d₆) δ 170.53, 148.03, 147.65, 141.85, 141.55, 140.96, 131.43, 129.78, 128.75, 128.70, 128.65, 124.66, 124.41, 118.83, 116.78, 44.71, 14.11.

Synthesis of EBT. SnCl₂ (1.273 g, 5.64 mmol) and ENBT (0.79 g, 1.71 mmol) were dissolved in 15 mL of methanol. The mixture was heated and stirred for 6 h at 70°C. The mixture was cooled to room temperature and the solvent was removed by rotary evaporator. The residue was purified by silica gel chromatography using dichloromethane: methanol (10:1) as eluent. The dark-colored oily compound EBT (0.34 g, 46%) was then obtained. ¹H NMR (400 MHz, DMSO-d₆) δ 8.32 (d, J = 7.6 Hz, 1H), 8.17 (d, J = 8.6 Hz, 1H), 8.01 (dd, J = 14.4, 11.1 Hz, 1H), 7.82 – 7.66 (m, 2H), 7.43 – 7.39 (m, 2H), 7.31 (d, J = 14.5 Hz, 1H), 7.19 – 7.07 (m, 1H), 6.63 (d, J = 8.6 Hz, 2H), 5.76 (s, 1H), 4.72 (q, J = 7.0 Hz, 2H), 4.02 (q, J = 7.1 Hz, 2H), 1.42 (t, J = 7.2 Hz, 3H). ¹³C NMR (151 MHz, Methanol-d₄) δ 153.90, 150.98, 132.11, 130.80, 130.31, 128.81, 128.36, 125.99, 124.48, 122.76, 116.37, 115.26, 111.31, 44.77, 13.72.

Spectrometric methods and solution preparation

11.60 mg ENBT and 10.85 mg EBT were dissolved in 25 mL of DMSO to prepare a 1.0 mM stock solution, respectively. Afterward, the solution was stored at 4°C for future use. For optical measurements, ENBT was diluted to 10 μM in PBS: DMSO (v/v = 99/1). Various concentrations of NTR and other analytes were then added and the change in fluorescence spectra of the reaction system was measured. The excitation wavelength was 515 nm. NADH was freshly prepared in ultrapure water (50 mM for stock solution, 500 μM for working concentration). 1 mg of NTR was dissolved in 1 mL of ultrapure water (to make a 1 mg/mL stock solution). They were packed in small centrifuge tubes and stored in a refrigerator at -20°C to prevent the enzyme activity from being affected by repeated access. Stock solutions of interfering substances for selectivity testing were freshly prepared in ultrapure water.

Determination of relative fluorescence quantum yield

The relative fluorescence quantum yield was calculated according to the following equation:

$$\Phi_s = \Phi_r \left(\frac{\eta_s}{\eta_r} \right)^2 \left(\frac{A_r}{A_s} \right) \left(\frac{F_s}{F_r} \right) \quad (1)$$

The subscripts *s* and *r* are the substance to be tested and the fluorescence

quantum yield standard, respectively, F is the integral area of fluorescence intensity, Φ is the fluorescence quantum yield, A is the absorbance, and η is the refractive index of the solvent. Quinine sulfate ($\Phi = 0.54$, 0.1 M H₂SO₄) and rhodamine B ($\Phi = 0.97$, ethanol) were chosen as standards for the determination of the relative fluorescence quantum yields of ENBT and EBT, respectively.

DFT Calculations

The calculations related to the properties of ENBT and EBT were implemented on the Gaussian 09 program. The time-dependent density functional theory (TD-DFT) with polarization function at a level of B3LYP/6-31 G (d) was applied as a method.

Docking Calculations

The binding affinity calculations between ENBT and NTR were carried out on AutoDock software (4.2.6 version). The NTR structure could be acquired from the Protein Data Bank, and the code is 4DN2. The docking results and figures were obtained on Ligplot+, AutoDock Vina, and PyMOL.

Cell culture and cell cytotoxicity assays

HeLa cells were grown in Dulbecco's modified Eagle's medium (DMEM) supplemented with 1% penicillin/streptomycin (P/S) and 10% fetal bovine serum (FBS) at 37 °C in 5% CO₂.

SH-SY5Y cells were grown in DMEM/Nutrient Mixture F-12 supplemented with 1% P/S and 15% FBS at 37 °C in 5% CO₂.

A549 cells were grown in Ham's F-12K (Kaighn's) supplemented with 1% P/S and 10% FBS at 37 °C in 5% CO₂.

HeLa cells were employed for in vitro cytotoxicity evaluation via the 3-(4,5-dimethylthiazol-2-yl)-2,5-diphenyltetrazolium bromide (MTT) assay. The cells were firstly transplanted in 96-well flat-bottomed plates for 24 h before incubation with ENBT for 24 h at concentrations of 0, 1, 5, 10, 20, and 40 μM. After that, the cells were rinsed with PBS 3 times and incubated with 0.5 mg·mL⁻¹ MTT in DMEM for 4 h at 37°C. Subsequently, the medium was discarded and the generated formazan was dissolved in 200 μL DMSO. The absorbance of the DMSO solution was then recorded by using a microplate reader at 490 nm.

Co-localization, photostability experiments and viscosity response.

HeLa cells were seeded into culture dishes and attached overnight. After the cells were attached, they were incubated for 6 h under hypoxic conditions. Subsequently, cells were added ENBT (10 μM) for 80 min, and afterward, cells were washed to get rid of the extra probe. Then the Mito-Tracker Green (200 nM) was added and co-incubated for 20 min. Afterward, cells were washed with PBS to acquire fluorescence imaging by using the CLSM. For the Mito Tracker Green channel, $\lambda_{\text{ex}} = 488$ nm, $\lambda_{\text{em}} = 505$ -540 nm; for the ENBT channel, $\lambda_{\text{ex}} = 559$ nm, $\lambda_{\text{em}} = 575$ -675 nm

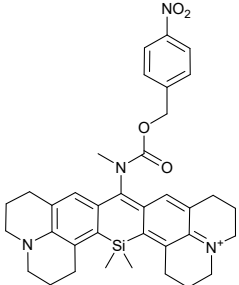
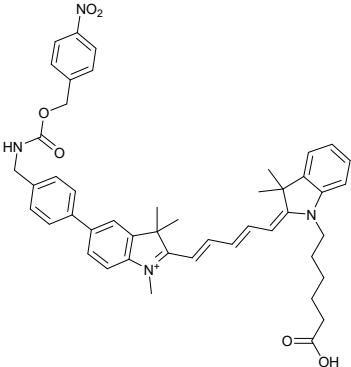
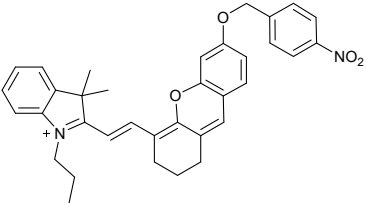
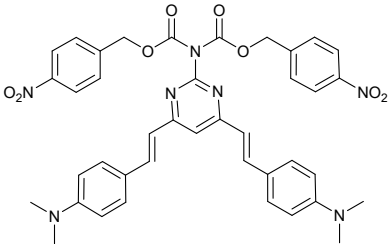
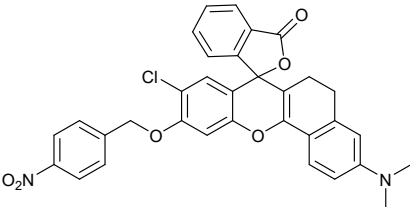
For the photostability assay, the time-dependent fluorescence images in the red channel were collected at $\lambda_{\text{ex}}/\lambda_{\text{em}} = 515/(605-680)$ nm. The images were simultaneously collected at 30 s intervals for 20 min on an FV-1100 CLSM with a 100× objective lens.

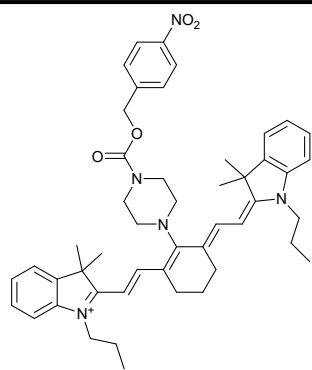
In addition, after culturing the cells under the hypoxic conditions and adding the probe, LPS (10 $\mu\text{g}/\text{mL}$) was then added to the cells. Then the fluorescence signal was observed in real-time with CLSM.

Bacteria culture and bacteria imaging

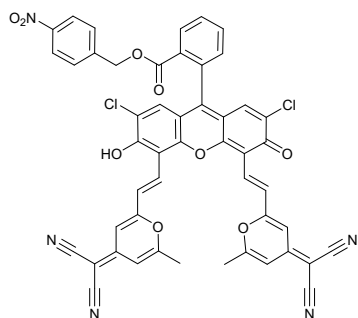
Staphylococcus aureus (*S. aureus*) was cultured in Luria-Bertani (LB) medium (1% w/v peptone, 0.5% w/v sodium chloride, 0.5% w/v yeast, pH 7.0-7.5) in a shaker at 37°C and 200 rpm for 6 h. The resulting bacterial solution was diluted to 10^7 colony-forming units per milliliter (CFU mL^{-1}) by PBS (0.01 M). This bacterial solution was co-incubated with ENBT (10 μM) for 2 h and then imaged by the CLSM. ($\lambda_{\text{ex}} = 515$ nm, $\lambda_{\text{em}} = 605-680$ nm).

Table S1. Some reported fluorescent probes for NTR.

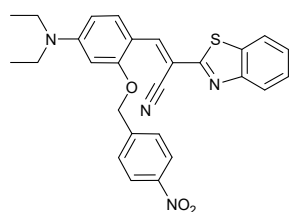
Probe structure	λ_{abs} (nm)	λ_{em} (nm)	Limit of detection (ng/mL)	References
	486/703	655/710	76	[1]
	645	670	32.9	[2]
	670	705	14	[3]
	400	520	16	[4]
	561	624	0.79	[5]



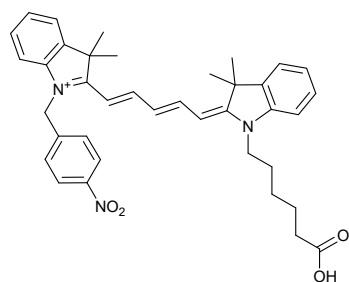
630 785 24.2 [6]



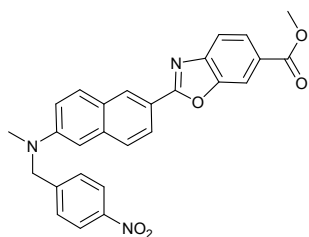
450-650 635 8 [7]



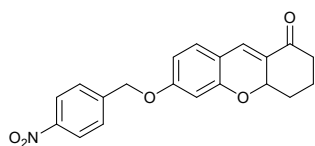
455 530 11 [8]



652 677 36.9 [9]



394 494 20 [10]



450 511 65 [11]

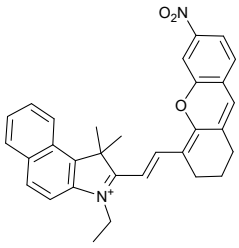
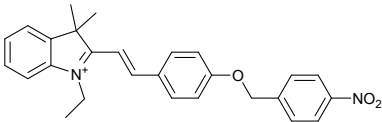
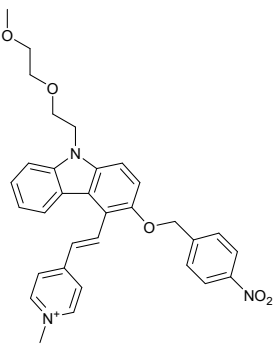
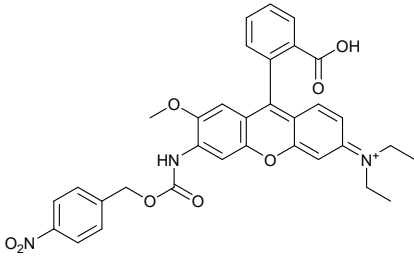
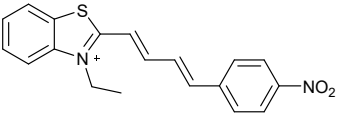
	630	670	720	0.096	[12]
	505	554	554	8.8	[13]
	450	535	535	13.8	[14]
	538	576	576	6.5	[15]
	475	664	664	36.8	This work

Table S2. Photo-physical properties of ENBT in water/glycerol (v/v) mixtures.

Glycerol/water	ε (M ⁻¹ cm ⁻¹)	Φ	$\varepsilon \times \Phi$ (M ⁻¹ cm ⁻¹)
0:10	24869	0.01	249
1:9	20963	0.01	210
3:7	23413	0.02	468
4:6	26486	0.02	530
6:4	24047	0.02	481
9:1	24180	0.05	1209
10:0	24647	0.05	1232

Table S3. Photo-physical properties of EBT in water/glycerol (v/v) mixtures.

Glycerol/water	ε (M ⁻¹ cm ⁻¹)	Φ	$\varepsilon \times \Phi$ (M ⁻¹ cm ⁻¹)
0:10	16934	0.02	339
1:9	10040	0.04	402
3:7	9970	0.04	399
4:6	10862	0.04	434
6:4	10951	0.07	767
9:1	10499	0.22	2310
10:0	10572	0.30	3172

ε is the extinction coefficient of probe at the maximum absorption, Φ is the relative fluorescence quantum yield, $\varepsilon \times \Phi$ represent for molecular brightness [16].

Table S4. Viscosity values in water/glycerol (v/v) mixtures at varied ratios [17].

Glycerol/water	η /cP (25°C)
0:10	0.89
1:9	1.15
2:8	1.54
3:7	2.16
4:6	3.18
5:5	5.04
6:4	8.82
7:3	17.96
8:2	45.86
9:1	163.60
10:0	945.00

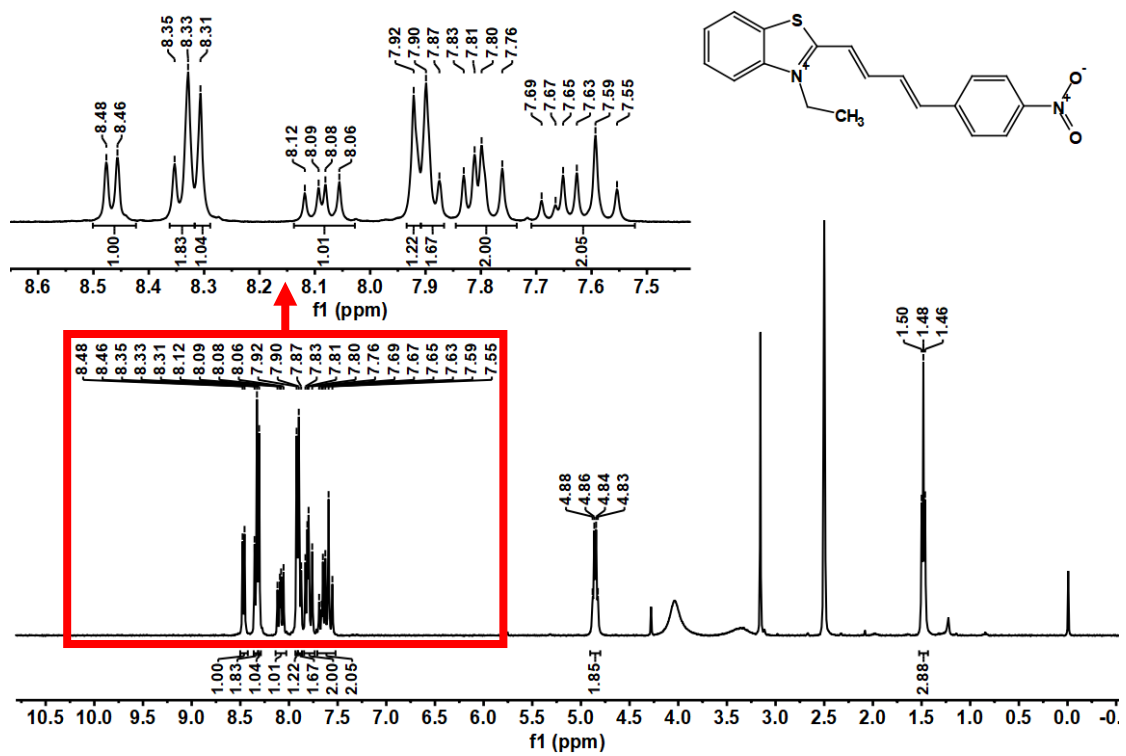


Figure S1. ^1H NMR spectra of ENBT in $\text{C}_2\text{D}_6\text{SO}$.

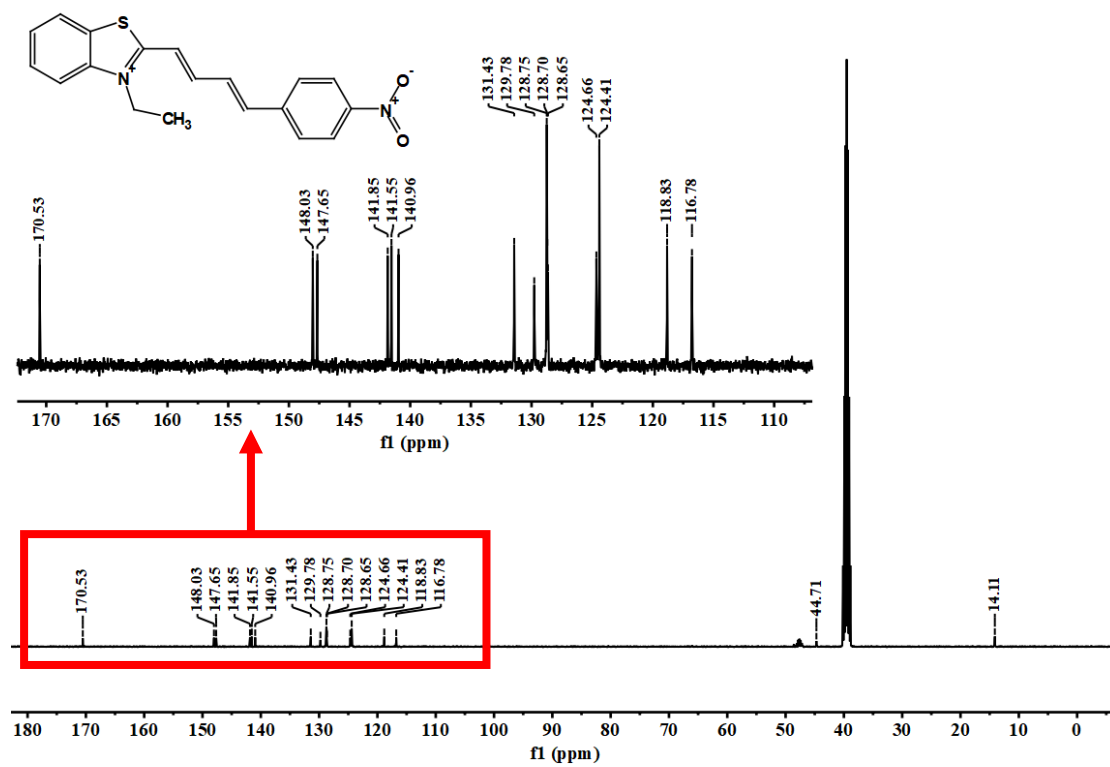


Figure S2. ¹³C NMR spectra of ENBT in C₂D₆SO.

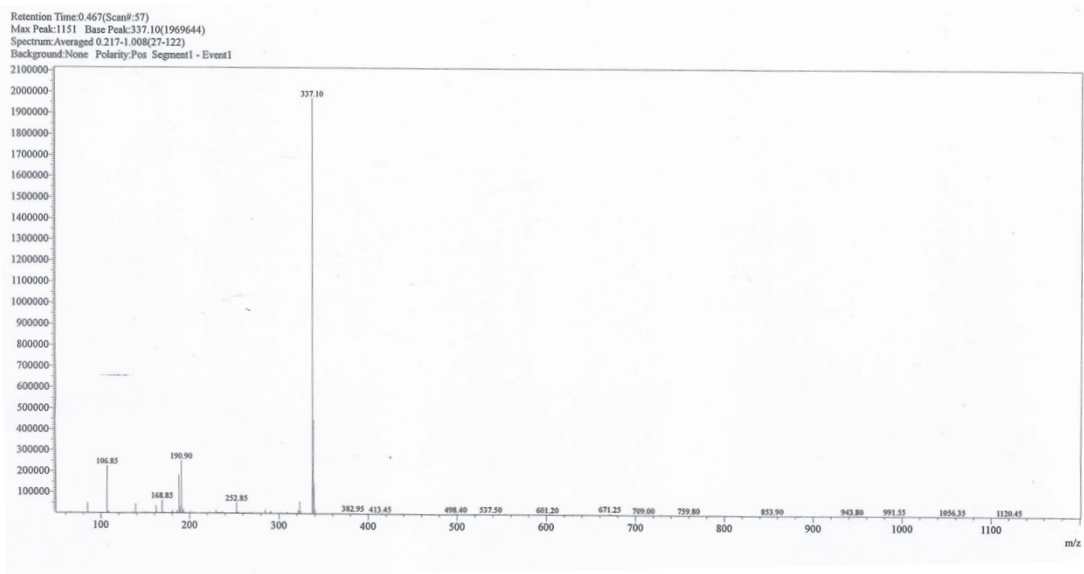


Figure S3. The Mass Spectra of ENBT (ESI).

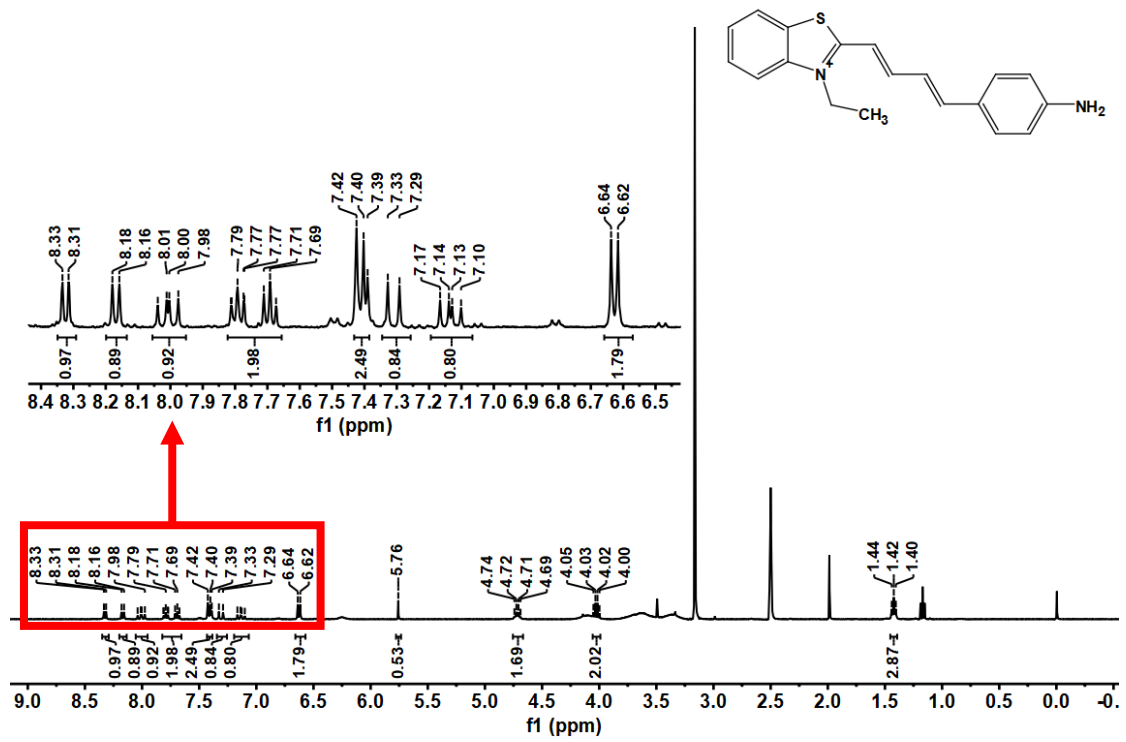


Figure S4. ^1H NMR spectra of EBT in $\text{C}_2\text{D}_6\text{SO}$.

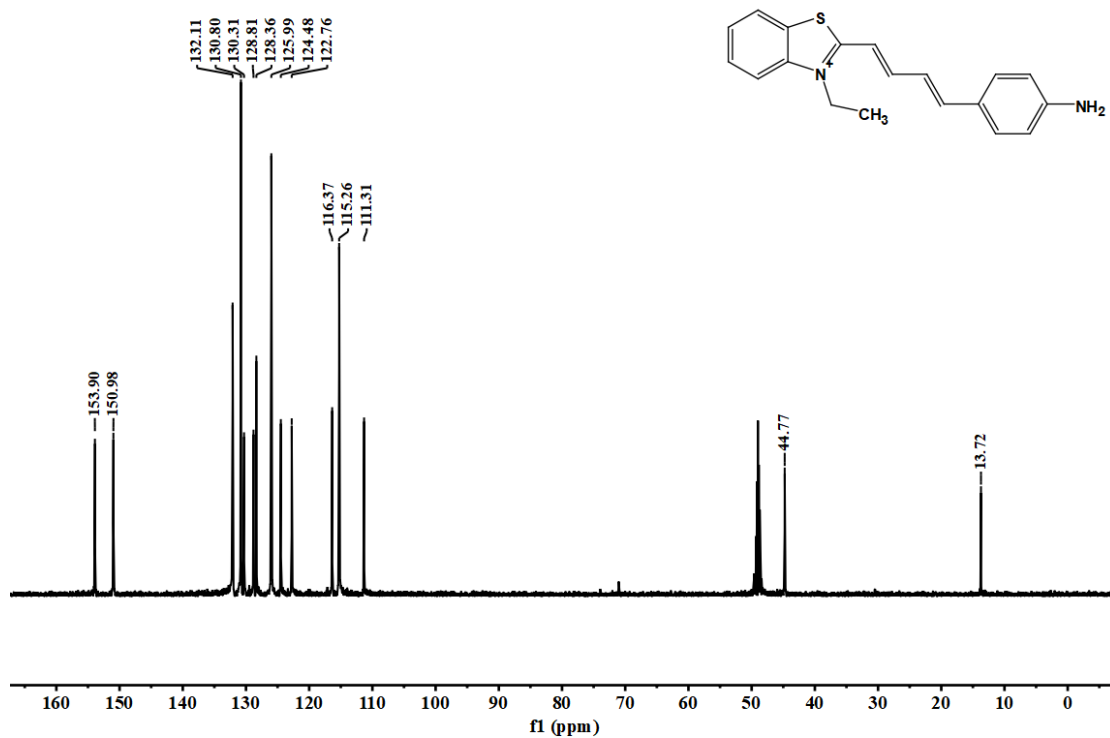


Figure S5. ^{13}C NMR spectra of EBT in CD_3OD .

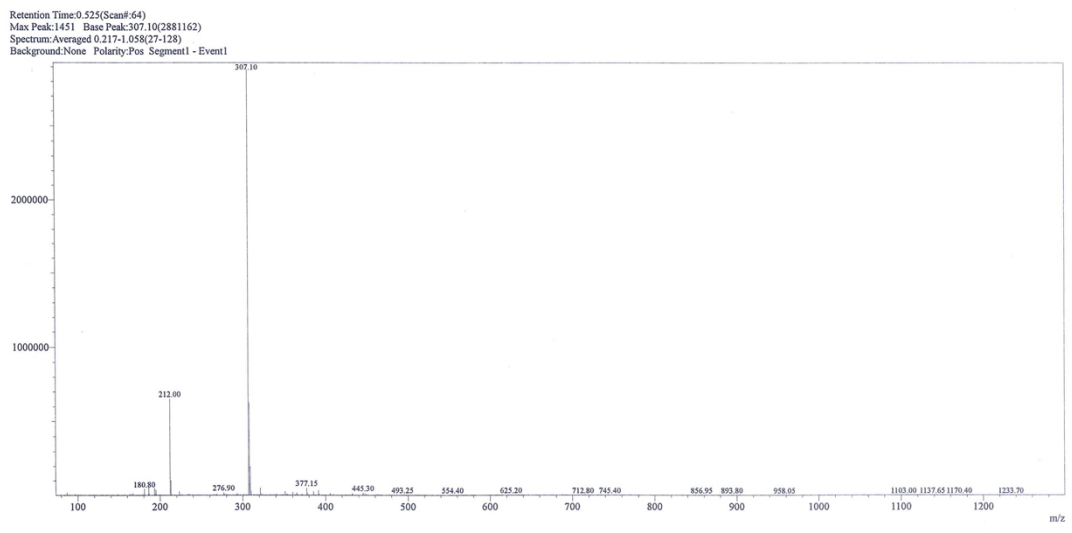


Figure S6. The Mass Spectra of EBT (ESI).

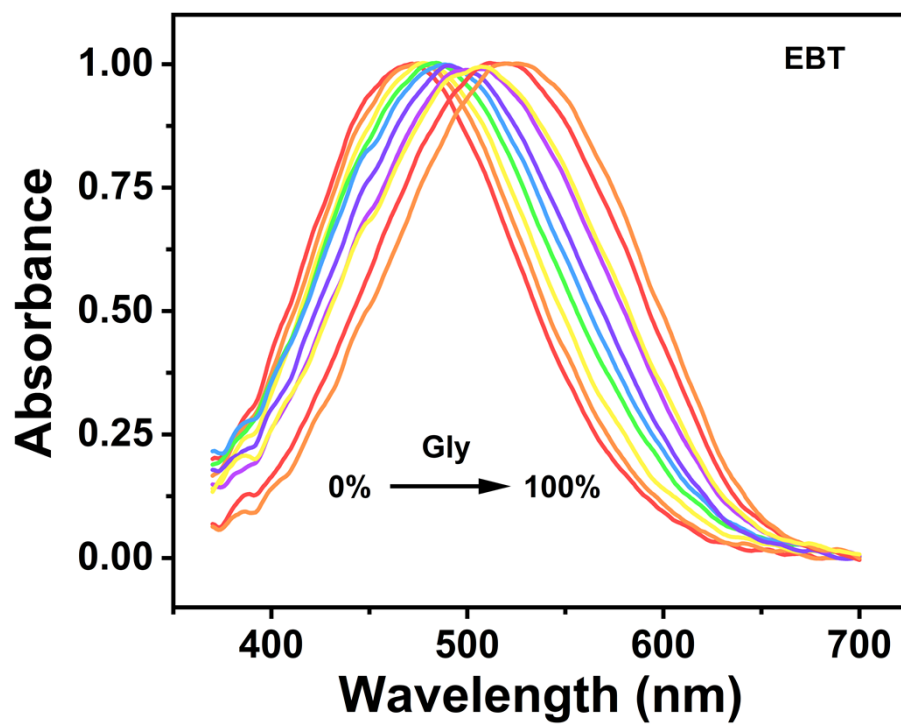


Figure S7. Ultraviolet-visible absorption spectra of EBT in 0%-100% glycerol.

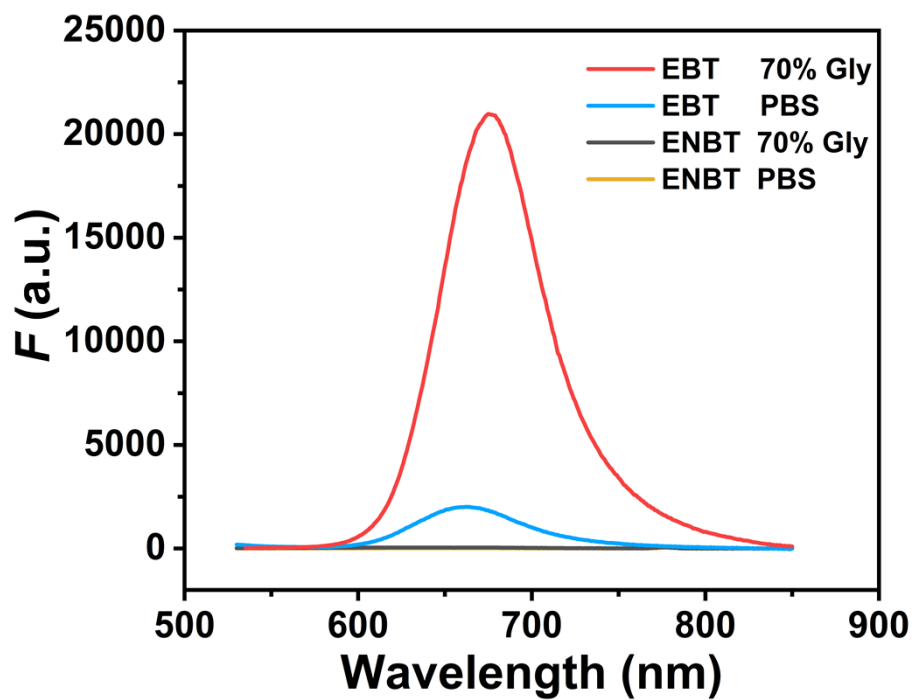


Figure S8. Fluorescence emission spectra of ENBT and EBT in PBS (pH 7.4) and glycerol (70%), respectively, $\lambda_{\text{ex}} = 515$ nm.

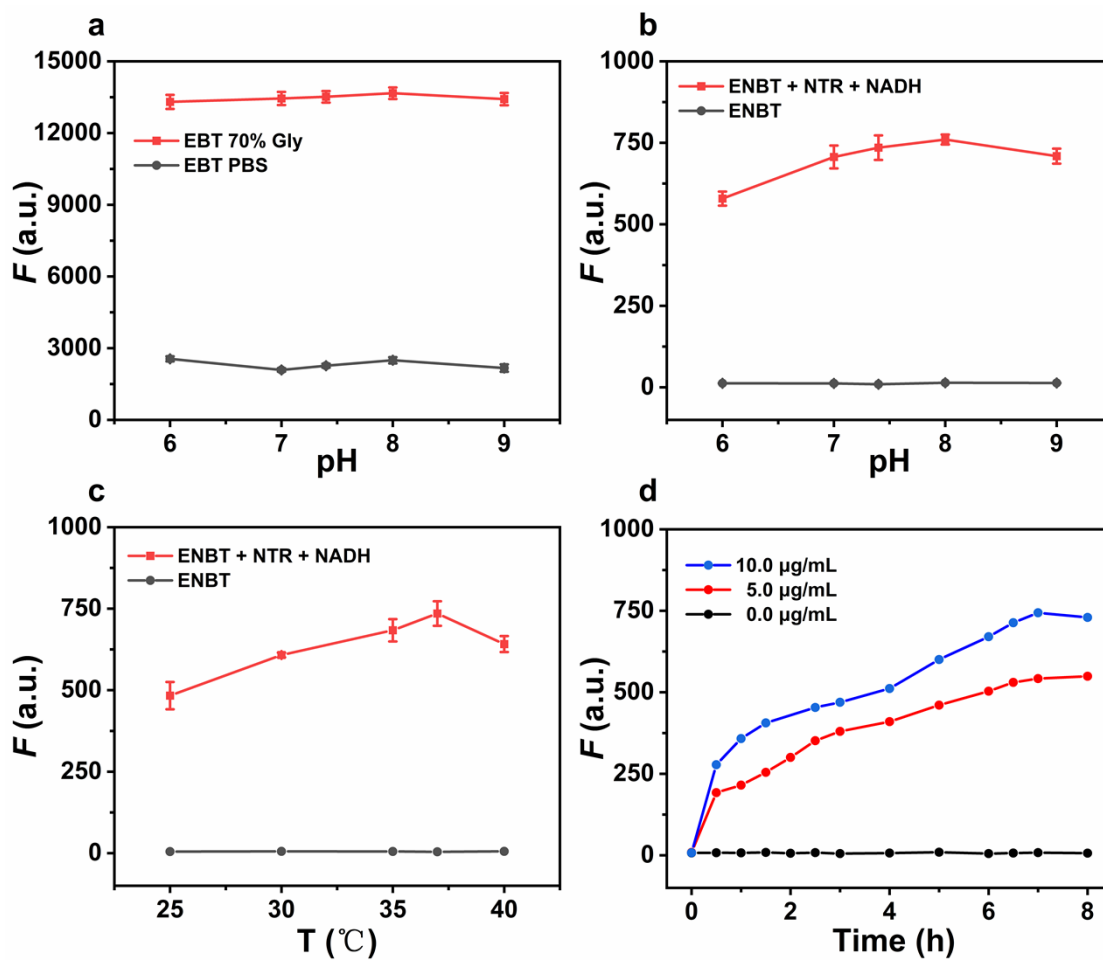


Figure S9. (a) fluorescence intensity of EBT at different pH (6.0-9.0); (b) fluorescence intensity of ENBT before and after reaction with NTR at different pH (6.0-9.0); (c) fluorescence intensity of ENBT before and after reaction with NTR at different temperature (25-40°C); (d) fluorescence intensity of ENBT (10 μM) at different time in reaction with NTR (0, 5.0, 10.0 μg/mL). $\lambda_{\text{ex}}/\lambda_{\text{em}} = 515/664$ nm.

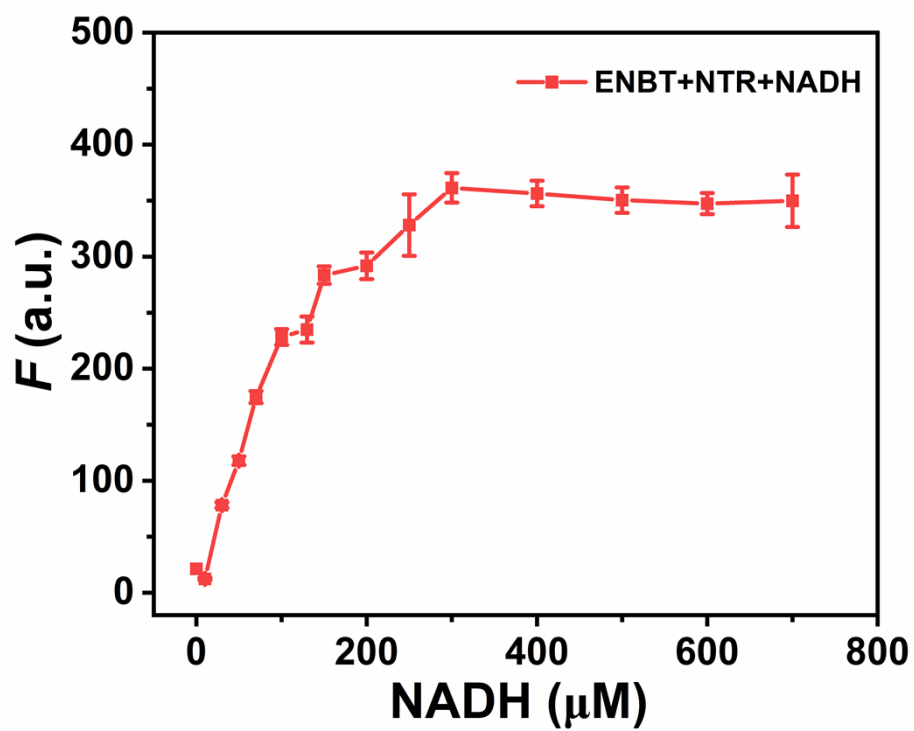


Figure S10. Effects of the concentration of NADH (0-700 μM) on ENBT (10 μM) upon addition of NTR (3 $\mu\text{g}/\text{mL}$) in PBS (pH 7.4). $\lambda_{\text{ex}}/\lambda_{\text{em}} = 515/664 \text{ nm}$.

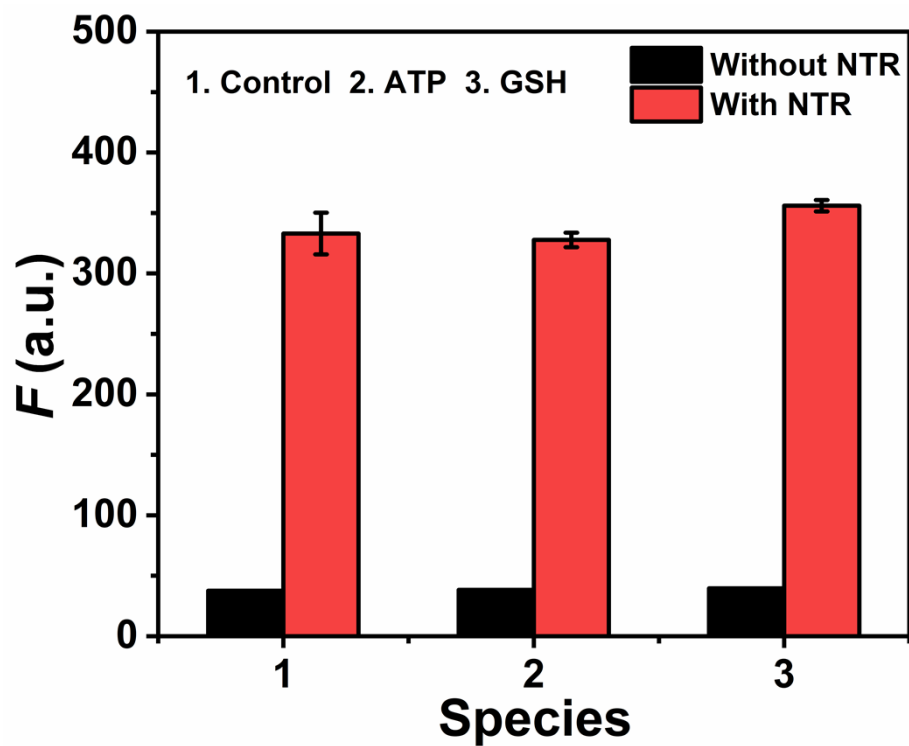


Figure S11. In the presence or absence of NTR (3 $\mu\text{g}/\text{mL}$), fluorescence intensity of ENBT (10 μM) after addition of ATP (10 mM) or GSH (10 mM) in PBS buffer (pH 7.4).

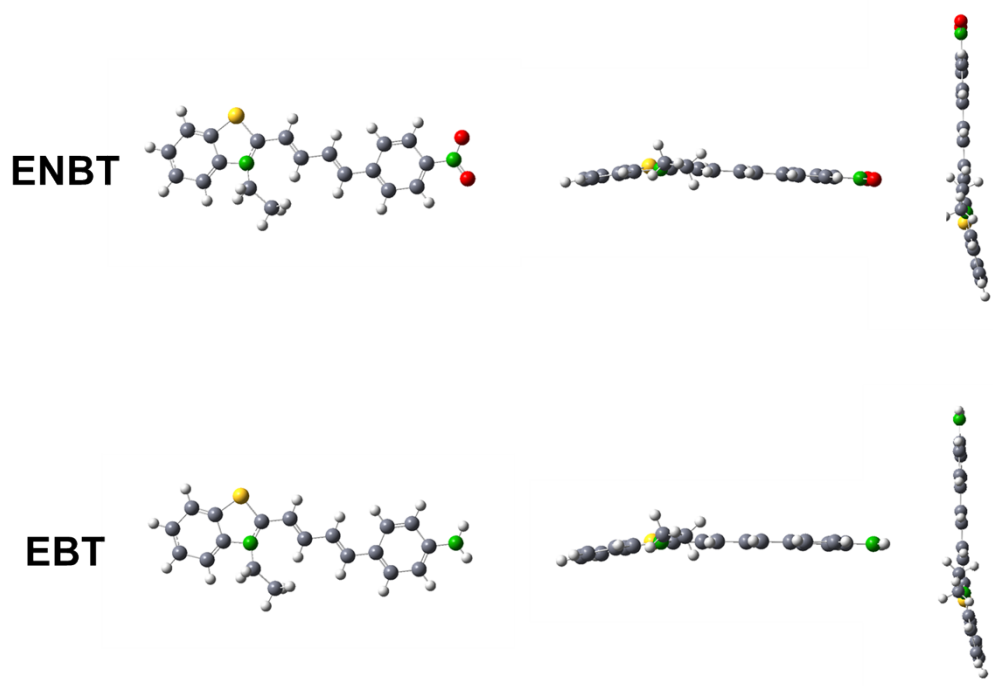


Figure S12. Energy-optimized geometries of ENBT and EBT.

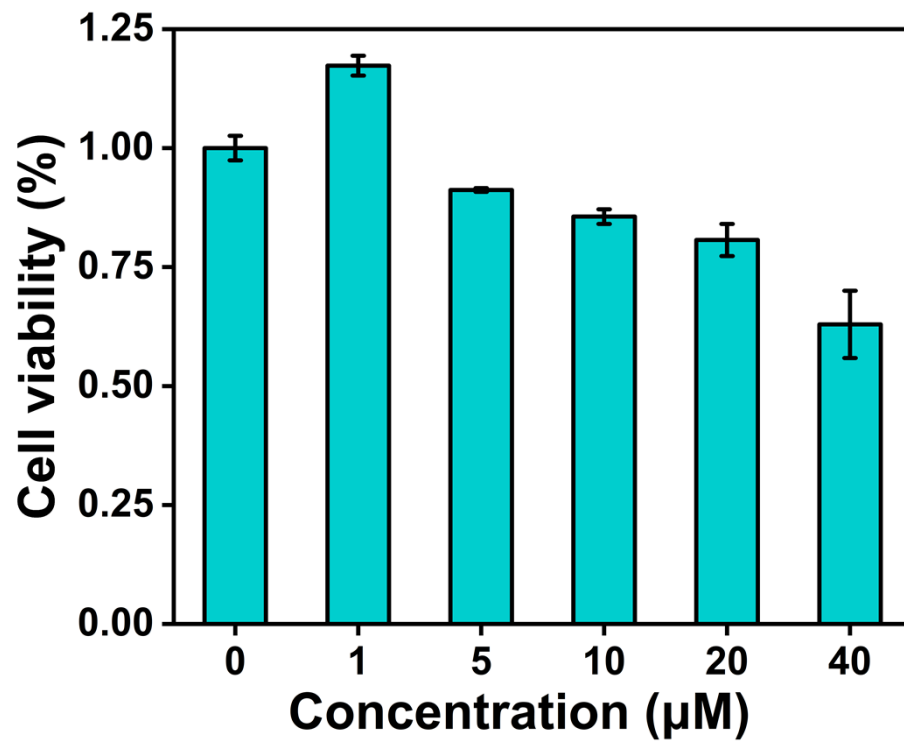


Figure S13. MTT assay of live HeLa cells in the presence of ENBT at various concentrations.

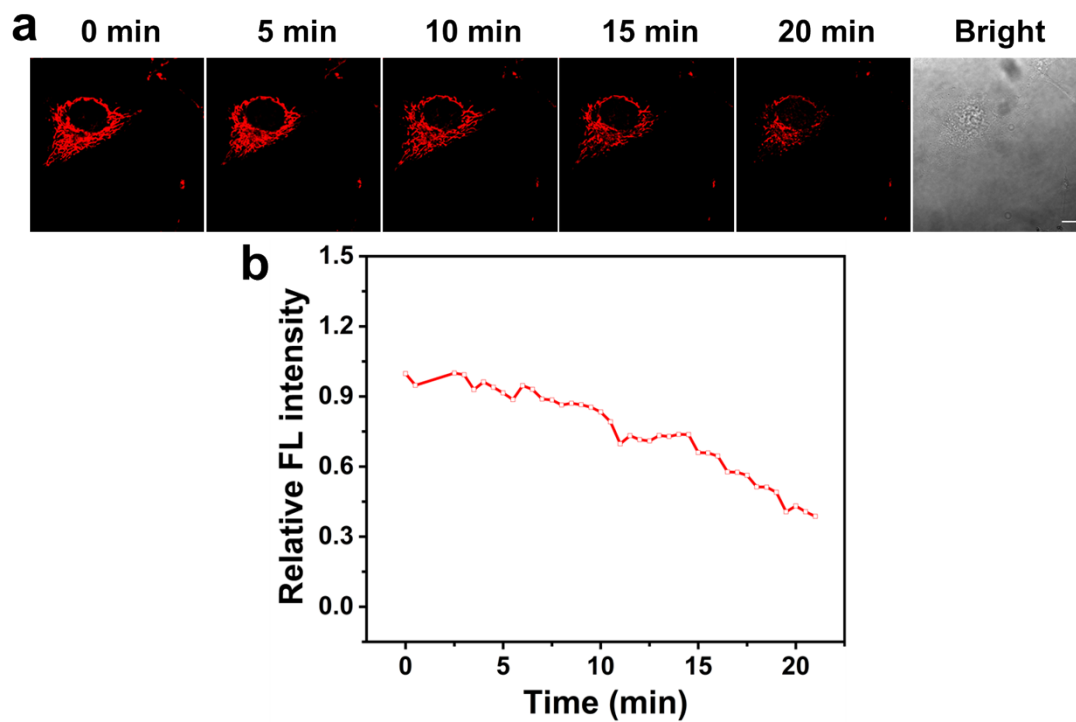


Figure S14. (a) The time-dependent fluorescence images of the dyes in live cells. (b) The relative fluorescence intensities from red channels in (a). $\lambda_{\text{ex}} = 515 \text{ nm}$, $\lambda_{\text{em}} = 605\text{-}680 \text{ nm}$. Scale bar = $10 \mu\text{m}$.

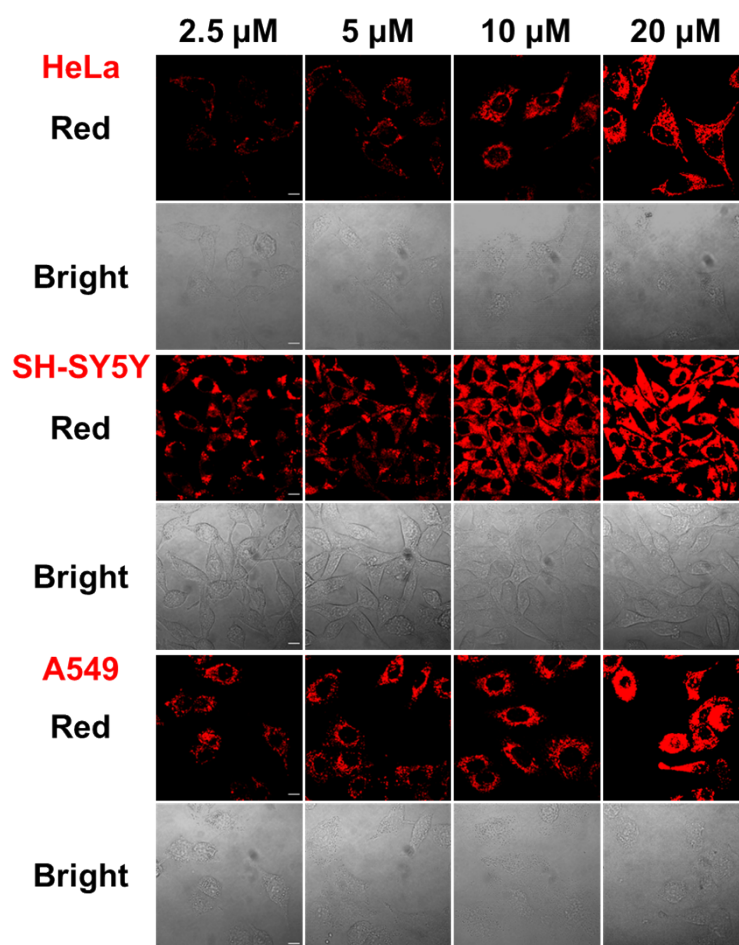


Figure S15. The fluorescence images of HeLa, SH-SY5Y, and A549 cells (cells grown under hypoxic conditions) incubated with different concentrations of ENBT. $\lambda_{\text{ex}} = 515 \text{ nm}$, $\lambda_{\text{em}} = 605\text{-}680 \text{ nm}$. Scale bar = 10 μm .

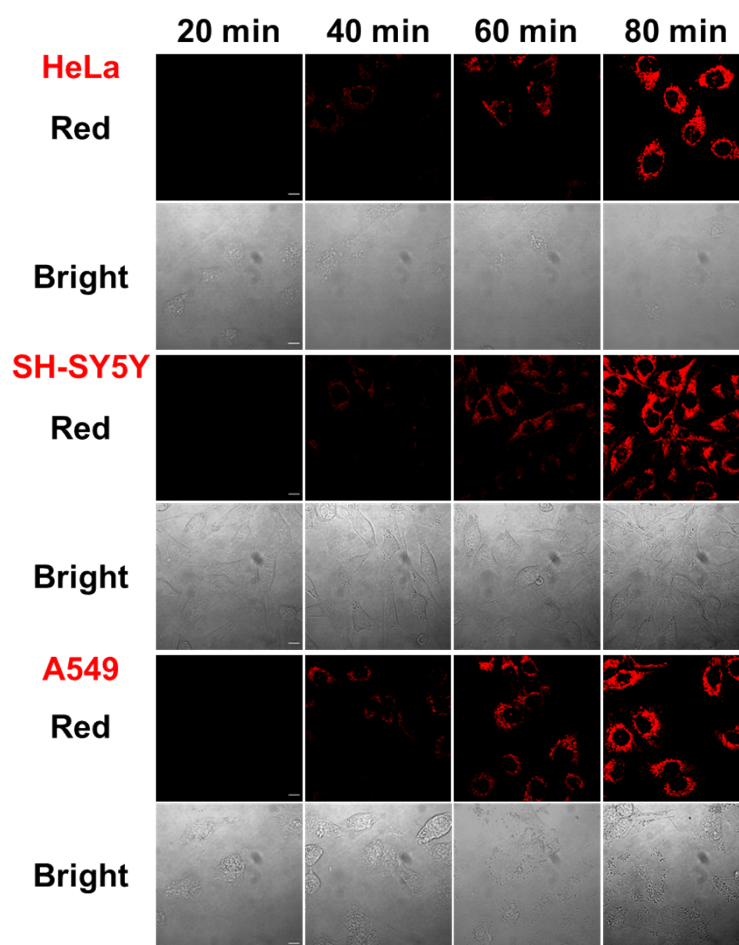


Figure S16. The fluorescence images of HeLa, SH-SY5Y, and A549 cells (cells grown under the hypoxic conditions) incubated with different periods of ENBT (10 μ M). $\lambda_{\text{ex}} = 515 \text{ nm}$, $\lambda_{\text{em}} = 605\text{-}680 \text{ nm}$. Scale bar = 10 μ m.

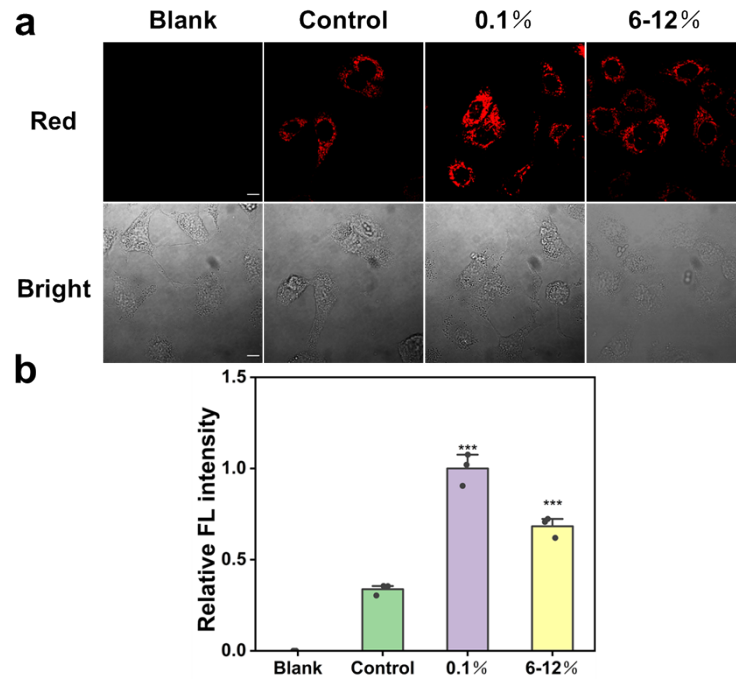


Figure S17. (a) Fluorescence imaging of A549 cells incubated with ENBT (10 μ M) under different conditions. First column: cells only, the second column: cells grown under the normoxic conditions (20% O₂, control), the third column: cells grown under the hypoxic conditions of 0.1% O₂, the fourth column: cells grown under the hypoxic conditions of 6-12% O₂. (b) The relative fluorescence intensities of A549 cells from red channels in (a). $\lambda_{\text{ex}} = 515 \text{ nm}$, $\lambda_{\text{em}} = 605\text{-}680 \text{ nm}$. Scale bar = 10 μ m.

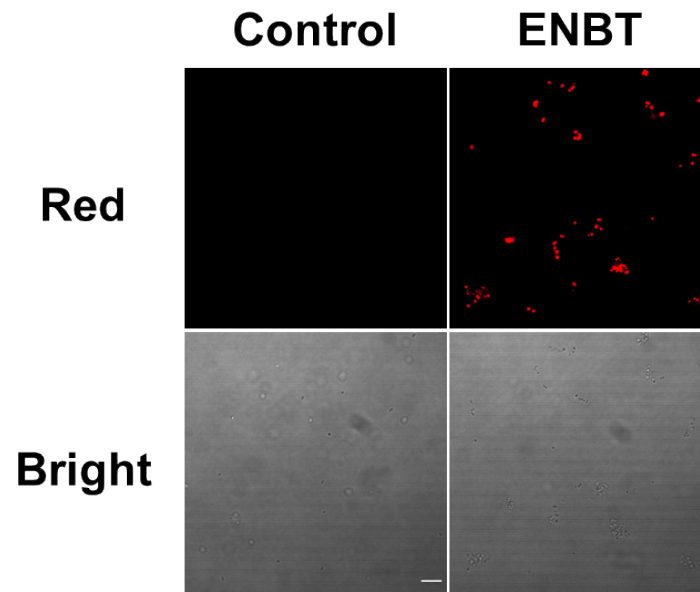


Figure S18. Fluorescence imaging of *S. aureus* incubated with ENBT (10 μ M). λ_{ex} = 515 nm, λ_{em} = 605-680 nm. Scale bar = 10 μ m.

Reference

- [1] Sarkar, S.; Lee, H.; Ryu, H. G.; Singha, S.; Lee, Y. M.; Reo, Y. J.; Jun, Y. W.; Kim, K. H.; Kim, W. J.; Ahn, K. H., A Study on Hypoxia Susceptibility of Organ Tissues by Fluorescence Imaging with a Ratiometric Nitroreductase Probe. *ACS Sens.* **2021**, *6* (1), 148-155.
- [2] Ji, Y. B.; Wang, Y. L.; Zhang, N.; Xu, S. N.; Zhang, L. L.; Wang, Q. H.; Zhang, Q. Y.; Hu, H. Y., Cell-Permeable Fluorogenic Probes for Identification and Imaging Nitroreductases in Live Bacterial Cells. *J. Org. Chem.* **2019**, *84* (3), 1299-1309.
- [3] Li, Z.; He, X. Y.; Wang, Z.; Yang, R. H.; Shi, W.; Ma, H. M., in vivo imaging and detection of nitroreductase in zebrafish by a new near-infrared fluorescence off-on probe. *Biosens. Bioelectron.* **2015**, *63*, 112-116.
- [4] Zhou, J.; Fang, S.; Zhang, D.; Qu, Y.; Wang, L.; Pan, S.; Li, L.; Li, J.; Du, W.; Wu, Q., A novel pyrimidine-based two-photon fluorogenic probe for rapidly visualizing nitroreductase activity in hypoxic cancer cells and in vivo. *Sens. Actuator B Chem.* **2023**, *390*.
- [5] Peng, R.; Yuan, J.; Cheng, D.; Ren, T. B.; Jin, F. P.; Yang, R. H.; Yuan, L.; Zhang, X. B., Evolving a Unique Red-Emitting Fluorophore with an Optically Tunable Hydroxy Group for Imaging Nitroreductase in Cells, in Tissues, and in Vivo. *Anal. Chem.* **2019**, *91* (24), 15974-15981.
- [6] Zheng, J. R.; Shen, Y. Z.; Xu, Z. Q.; Yuan, Z. W.; He, Y. Y.; Wei, C.; Er, M.; Yin, J.; Chen, H. Y., Near-infrared off-on fluorescence probe activated by NTR for in vivo hypoxia imaging. *Biosens. Bioelectron.* **2018**, *119*, 141-148.
- [7] Liu, Z. W.; Song, F. L.; Shi, W. B.; Gurzadyan, G.; Yin, H. Y.; Song, B.; Liang, R.; Peng, X. J., Nitroreductase-Activatable Theranostic Molecules with High PDT Efficiency under Mild Hypoxia Based on a TADF Fluorescein Derivative. *ACS Appl. Mater. Interfaces* **2019**, *11* (17), 15426-15435.
- [8] Xia, L. L.; Hu, F.; Huang, J. X.; Li, N.; Gu, Y. Q.; Wang, P., A fluorescent turn-on probe for nitroreductase imaging in living cells and tissues under hypoxia conditions. *Sens. Actuator B Chem.* **2018**, *268*, 70-76.
- [9] Zhang, N.; Wang, Y. L.; Leng, S.; Xu, S. N.; Zhang, L. L.; Wang, Q. H.; Zhang, Q. Y.; Hu, H. Y., An efficient fluorescence sensor for nitroreductase selective imaging based on intramolecular photoinduced electron transfer. *Talanta* **2019**, *205*, 7.
- [10] Zhang, J.; Liu, H. W.; Hu, X. X.; Li, J.; Liang, L. H.; Zhang, X. B.; Tan, W. H., Efficient Two-Photon Fluorescent Probe for Nitroreductase Detection and Hypoxia Imaging in Tumor Cells and Tissues. *Anal. Chem.* **2015**, *87* (23), 11832-11839.
- [11] Liu, Z. R.; Tang, Y. H.; Xu, A.; Lin, W. Y., A new fluorescent probe with a large turn-on signal for imaging nitroreductase in tumor cells and tissues by two-photon microscopy. *Biosens. Bioelectron.* **2017**, *89*, 853-858.
- [12] Wang, S.; Zhang, X.-F.; Wang, H.-S.; Liu, J.; Shen, S.-L.; Cao, X.-Q., A highly sensitive NIR fluorescence probe for hypoxia imaging in cells and ulcerative colitis. *Talanta* **2023**, *252*.
- [13] Zhang, L.; Zhang, L.; Zhang, X.; Liu, P.; Wang, Y.; Han, X.; Chen, L., Fluorescent imaging to provide visualized evidences for mercury induced hypoxia stress. *J. Hazard. Mater.* **2023**, *444*, 130374.
- [14] Wen, L.; Shao, M.; Li, Y.; Zhang, Y.; Peng, C.; Yu, H.; Zhang, K., Unveiling the hypoxia-induced mitophagy process through two-channel real-time imaging of NTR and viscosity under the same excitation. *Talanta* **2024**, *266*.

- [15] Guo, H.; Yang, K.; Fan, X.; Chen, M.; Ke, G.; Ren, T.-B.; Yuan, L.; Zhang, X.-B., Designing a Brightness-Restored Rhodamine Derivative by the Ortho-Compensation Effect for Assessing Drug-Induced Acute Kidney Injury. *Anal. Chem.* **2023**, *95* (17), 6863-6870.
- [16] Grimm, J. B.; Lavis, L. D., Caveat fluorophore: an insiders' guide to small-molecule fluorescent labels. *Nat. Methods* **2021**, *19* (2), 149-158.
- [17] Xu, W.; Liu, S.; Chen, Z.; Wu, F.; Cao, W.; Tian, Y.; Xiong, H., Bichromatic Imaging with Hemicyanine Fluorophores Enables Simultaneous Visualization of Non-alcoholic Fatty Liver Disease and Metastatic Intestinal Cancer. *Anal. Chem.* **2022**, *94* (39), 13556-13565.